Struct Multidisc Optim 19, 64–73

Structural design using cellular automata

E. Kita and T. Toyoda

Abstract This paper presents a shape and topology optimization scheme for structures by using the concept of a cellular automaton (CA). A design domain is divided into small square cells and then the thicknesses of the individual cells are taken as the design variables. Considering the cells as the finite elements, the stress analysis is performed by the finite element method. The design variables are modified by applying a local rule to the stress states of the cell and its neighbouring cells. The present scheme is applied to a two-dimensional elastic problem in order to confirm its validity.

1 Introduction

A self-reproduction automaton was first presented by Von Neumann. Following Ulam's suggestions, he reformulated it to what would be known as the first cellular automaton (CA) (Levy 1992; Waldrop 1992) The cellular automaton is considered a discrete simulation scheme. The domain occupied by the object under consideration and the time are discretized with physical quantities usually taken on the set of the finite values. A cellular automaton consists of regular square cells with discrete variables. The quantities at each cell are updated simultaneously based on the quantities of the cell and its neighbouring cells at the preceding step and according to a definite set of "local rules". Since the local rule is defined so as to govern only local relationships among the neighbouring cells, the governing equation for the whole domain is not necessary. Therefore, the cellular automaton is considered to be very effective for simulating physical phenomena whose governing equations are unknown. Many researchers have been applying the cellular automaton to the simulation of different phenomena such as, for example, the traffic flow, the diffusion phenomena of the particles and the liquid flow (Doolen *et al.* 1987; Eissler *et al.* 1992; Clayton 1993; Wolfram 1994; Garzon 1995; Gaylord and Nishidate 1996) This paper considers the application of the cellular automaton to the optimal design of two-dimensional structures.

The application of the cellular automaton to shape optimization of structures has already been presented by Inou *et al.* (1994, 1998), Kundu *et al.* (1997a,b), Tada *et al.* (1995), Xie and his colleagues (Xie and Steven 1993, 1994a,b, 1996; Zhao *et al.* 1997, 1998; Yang *et al.* 1998; Kim *et al.* 1998; Young *et al.* 1998; Guan *et al.* 1998; Chu *et al.* 1998; Nha *et al.* 1998), and others (Umetani and Hirai 1975; Chaudouet-Miranda and El Yafi 1987; Payten *et al.* 1998; Payten and Law 1998; Payten 1998).

The basic idea was described by Inou *et al.* (1994, 1998). In those papers, the design domain is divided into many small cells and the von Mises equivalent stress distribution on the whole domain is estimated by the finite element method. Then, the reference stress which is individually specified at each cell is updated by applying a local rule to the stress distribution. Young's modulus for each cell is taken as a design variable, which is modified so that the equivalent stress at the updated cell is to be equal to the reference stress. The cells with relative small Young's modulus are removed and therefore, the shape and topology of the structures are modified. The local rule in this study is defined as the nonlinear relationship between the equivalent stress distribution and Young's modulus. Since the local rule is derived from the numerical experience, the mathematical relationship between the rule and the optimization problem is not obvious. Also, since the reference stress for each cell is individually modified by the local rule during iterative process, it may be difficult to introduce the stress constraint conditions to the optimization problem.

On the other hand, Xie and his colleagues presented the evolutionary structural optimization (ESO) scheme (Xie and Steven 1993, 1994a, 1996; Zhao *et al.* 1997; Kim *et al.* 1998). In this scheme, the reference value is firstly specified. After the stress analysis by the finite element method, one removes the cells where the stresses are smaller than the reference value. In their newer studies, the ESO scheme was extended to the bi-directional evolu-

Received October 8, 1998
Revised manuscript received January 18, 1999

E. Kita and T. Toyoda

Department of Mechano-Informatics & Systems, Nagoya University, Nagoya 464–8603, Japan

tionary structural optimization (BESO) scheme (Yang *et al.* 1998; Young *et al.* 1998). In this scheme, two reference values are introduced. Some cells are removed according to the first reference value, while other cells can be added. The physical meaning of the reference values, however, is not obvious and therefore, should be specified according to numerical experiments or users' experiences.

To overcome the above difficulties, we present the following algorithm. The design domain is divided into small square cells and the thicknesses of the cells are taken as the design variables. The optimization problem for the whole structure is reformulated as the individual optimization problem for each cell by introducing special constraint conditions, so-called "CA-constraint condition". The functional of the problem is analytically defined and the local rule can be derived by setting the first variation of the functional equal to zero. Since, in this case, the reference stress at each cell is not changed by the local rule, it is easy to add the stress constraint conditions to the optimization problem. Moreover, the formulation does not include the new parameters, whose physical definition is not clear.

This paper is organized as follows. In Section 2, the cellular expression of structures and the finite element formulation for the two-dimensional elastic problem are described briefly. In Section 3, the derivation of the local rule is explained in detail. In Section 4, the present scheme is applied to the topology and shape optimization problem of a two-dimensional elastic body. Finally, Section 5 summarizes some conclusions.

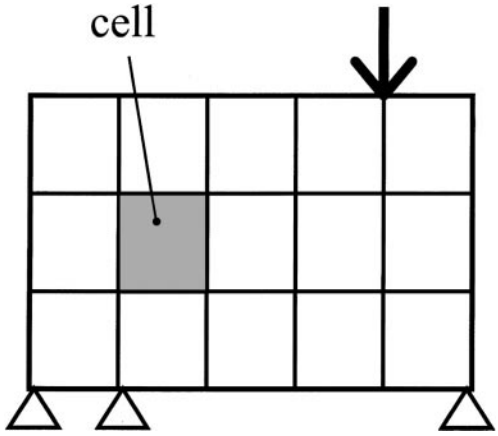

Fig. 1 Design domain

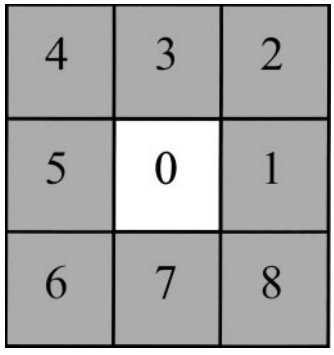

Fig. 2 Moor neighbourhood

2
Cellular automaton and the finite element method

2.1
Cellular expression of structures

The design domain is typically divided into small square subdomains (Fig. 1). The subdomains are considered as the elements and then, the stress distribution on the whole structure is estimated by the finite element method. The subdomains act as the cells in the cellular automaton simulation. In the usual cellular automaton simulation, the physical quantity or the function of each cell is taken on the set of the finite values. In this study, however, the functions are described by continuous ones.

The function of each cell is updated simultaneously based on the function values of the cell and the neighbouring cells at the preceding step and according to a local rule. Figure 2 shows the neighbourhood relationship among the cells. The cell 0 denotes the cell whose function is to be updated and the neighbouring cells are indicated as the cells 1 to 8. If the cell 0 is on the boundary, some of the neighbouring cells, of course, do not exist and therefore, in such a case, only existing cells are considered as neighbouring cells.

2.2
Finite element method

We explain the finite element formulation briefly so that the derivation of the local rule in the next section may easily be understood (Bathe 1982; Zienkiewicz and Taylor 1991).

The principle of the virtual work without the body forces is given as

$$\int_{\Omega} \delta\boldsymbol{\varepsilon}^T \boldsymbol{\sigma} \mathrm{d}\,\Omega = \int_{\Gamma_t} \delta\mathbf{u}^T \overline{\mathbf{t}} \mathrm{d}\,\Gamma\,, \tag{1}$$

where Ω, Γ_u and Γ_t, respectively, denote the domain occupied by the object under consideration, its displacement- and traction-specified boundaries and the whole boundary $\Gamma = \Gamma_u \bigcap \Gamma_t$. The vectors $\mathbf{u}, \mathbf{t}, \boldsymbol{\varepsilon}$ and $\boldsymbol{\sigma}$ respectively denote the vectors of the displacement, traction, strain and stress components in the two-dimensional elastic problem. The symbol δ and the superscript T, respectively, denote the virtual changes and the transpose of the matrix or vector. The relationship between the displacement and the strain components are given as

$$\boldsymbol{\varepsilon} = \mathbf{A}\mathbf{u}\,, \tag{2}$$

where $\mathbf{A}$ is defined as

$$\mathbf{A} = \begin{bmatrix} \partial/\partial x_1 & 0 \\ 0 & \partial/\partial x_2 \\ \partial/\partial x_2 & \partial/\partial x_1 \end{bmatrix} . \tag{3}$$

The relationship between the strain and the stress components are given as

$$\boldsymbol{\sigma} = \mathbf{D}\boldsymbol{\varepsilon} , \tag{4}$$

where $\mathbf{D}$ is defined as

$$\mathbf{D} = \frac{E}{1-\nu^2} \begin{bmatrix} 1 & \nu & 0 \\ \nu & 1 & 0 \\ 0 & 0 & (1-\nu)/2 \end{bmatrix} , \tag{5}$$

where E and ν, respectively, denote the Young's modulus and Poisson's ratio of the material. The relationship between the stress and the traction components are

$$t_i = \sigma_{ij} n_j , \tag{6}$$

where n_j denotes the x_j-component of the outer normal vector on the boundary.

Discretizing the left-hand side of (1) into N_e finite elements, we have

$$\int_{\Omega} \delta\boldsymbol{\varepsilon}^T \boldsymbol{\sigma} \mathrm{d}\,\Omega = \sum_{e=1}^{N_e} \int_{\Omega_e} \delta\boldsymbol{\varepsilon}_e^T \boldsymbol{\sigma}_e \mathrm{d}\,\Omega . \tag{7}$$

The displacement components at element e are approximated by the interpolation functions $\mathbf{N}$ with the nodal displacements $\mathbf{U}_e$,

$$\mathbf{u}_e = \mathbf{N}\mathbf{U}_e . \tag{8}$$

The stress and the strain components may then be expressed as

$$\boldsymbol{\varepsilon}_e = \mathbf{A}\mathbf{u}_e = \mathbf{A}\mathbf{N}\mathbf{U}_e \equiv \mathbf{B}\mathbf{U}_e , \tag{9}$$

and

$$\boldsymbol{\sigma}_e = \mathbf{D}\boldsymbol{\varepsilon}_e = \mathbf{D}\mathbf{B}\mathbf{U}_e . \tag{10}$$

Substituting the above approximate expressions into (7) gives

$$\int_{\Omega} \delta\boldsymbol{\varepsilon}^T \boldsymbol{\sigma} \mathrm{d}\,\Omega = \sum_{e=1}^{N_e} \int_{\Omega_e} \delta\boldsymbol{\varepsilon}_e^T \boldsymbol{\sigma}_e \mathrm{d}\,\Omega =$$

$$\sum_{e=1}^{N_e} \int_{\Omega_e} (\mathbf{B}\delta\mathbf{U}_e)^T \mathbf{D}\mathbf{B}\mathbf{U}_e \mathrm{d}\,\Omega \equiv \sum_{e=1}^{N_e} \delta\mathbf{U}_e^T h_e \mathbf{K}'_e \mathbf{U}_e , \tag{11}$$

where h_e and $\mathbf{K}'_e$, respectively, denote the thickness and the stiffness matrix at the element e.

Discretizing the right-hand side of (1) by N_ℓ boundary elements gives

$$\int_{\Gamma_t} \delta\mathbf{u}^T \overline{\mathbf{t}} \mathrm{d}\,\Gamma = \sum_{\ell=1}^{N_\ell} \int_{\Gamma_{t_\ell}} (\mathbf{N}\delta\mathbf{U})^T \overline{\mathbf{t}} \mathrm{d}\,\Gamma \equiv \sum_{\ell=1}^{N_\ell} \delta\mathbf{U}_\ell^T \mathbf{f}'_\ell , \tag{12}$$

where $\mathbf{f}'_\ell$ denotes the equivalent nodal force vector at the boundary element ℓ.

Substituting (11) and (12) into (1) gives

$$\sum_{e=1}^{N_e} \delta\mathbf{U}_e^T h_e \mathbf{K}'_e \mathbf{U}_e = \sum_{\ell=1}^{N_\ell} \delta\mathbf{U}_\ell^T \mathbf{f}'_\ell , \tag{13}$$

and

$$\delta\mathbf{U}^T \mathbf{K}\mathbf{U} = \delta\mathbf{U}^T \mathbf{f} , \quad \mathbf{K}\mathbf{U} = \mathbf{f} , \tag{14}$$

where $\mathbf{K}$ and $\mathbf{f}$, respectively, denote the global stiffness matrix and the global equivalent nodal force vector.

3 Derivation of the local rule

3.1 Optimization problem

The objectives of the design optimization problem are to minimize both the total weight of structures and the deviation between the yield stress of the material and the von Mises equivalent stress at the cells. The cell thicknesses are taken as the design variables. Further, in order to formulate the optimization problem for each element individually, we introduce a special constraint condition, the so-called "CA-constraint condition". This CA-constraint condition is defined so as to minimize the variation of the equivalent stress of the neighbouring cells with respect to the variation of the thickness of the updated cell.

3.1.1 Objective function 1

The first objective is to minimize the weight of the updated cell. If the area of the cell and the material are invariant, the objective function can be defined as

$$W_1 = h^2 , \tag{15}$$

where h denotes the thickness of the updated cell divided by the initial thickness of the cell.

3.1.2
Objective function 2

The second objective is to minimize the stress deviation, which can be defined as

$$W_2 = \left(\frac{\tilde{\sigma}_0}{\sigma_c} - 1\right)^2 \equiv (\sigma_0 - 1)^2 \,, \tag{16}$$

where $\tilde{\sigma}_0$ and σ_c, respectively, denote the von Mises equivalent stress at the updated cell and the yield stress of the material.

3.1.3
CA-constraint condition

The CA-constraint conditions are defined as

$$g_i = \frac{\tilde{\sigma}_i}{\tilde{\sigma}_i^0} - 1 \equiv \sigma_i - 1 = 0 \quad (i = 1, \ldots, 8) \,, \tag{17}$$

where $\tilde{\sigma}_i$ and $\tilde{\sigma}_i^0$, respectively, denote the equivalent stresses at the neighbouring cell i at the present and the preceding steps. Therefore, (17) ensures that the variation of the equivalent stress at the neighbouring cell is small.

3.2
Multicriteria optimization problem

If both the above objectives are to be achieved in some sense, a new objective function W_3 is defined as the weighted sum of the above objective functions given by

$$W_3 = \alpha W_1 + \beta W_2 \,, \tag{18}$$

where α and β are weight parameters satisfying the condition

$$\alpha + \beta = 1 \,, \tag{19}$$

where

$$\beta = \begin{cases} \sigma_0 & (\sigma_0 < 1) \\ 1 & (\sigma_0 \geq 1) \end{cases} . \tag{20}$$

The weight parameters set the relative importance of the objective functions according to the magnitude of σ_0. If $\sigma_0 \geq 1$, $\beta = 1$, $\alpha = 0$ and therefore the objective function to be minimized is

$$W_3 = W_2 = (\sigma_0 - 1)^2 \,,$$

i.e. in this case, the shape optimization is performed so as to minimize the stress deviation. On the other hand, if σ_0 is relatively small, $\alpha \simeq 1$, $\beta \simeq 0$ and therefore the objective function becomes

$$W_3 \simeq W_1 = h^2 \,,$$

i.e. in this case, the shape optimization is performed so as to minimize the weight.

By adding the constraint condition (17) multiplied by the penalty parameter p to (18), we have the penalty function W,

$$W = \alpha W_1 + \beta W_2 + p \sum_{i=1}^{8} g_i^2 =$$

$$\alpha h^2 + \beta(\sigma_0 - 1)^2 + p \sum_{i=1}^{8} (\sigma_i - 1)^2 \,. \tag{21}$$

By expanding the equivalent stress σ_i around $h + \delta h$, we have

$$\sigma_i(h + \delta h) \simeq \sigma_i(h) + \acute{\sigma}_i \delta h \quad (i = 0, \ldots, 8) \,, \tag{22}$$

where $(\acute{}) = \partial/\partial h$. By using the above equation, we can derive the Taylor's expansion representation of (21),

$$W(h + \delta h) \simeq \alpha(h + \delta h)^2 + \beta(\sigma_0 + \acute{\sigma}_0 \delta h - 1)^2 +$$

$$p \sum_{i=1}^{8} (\sigma_i + \acute{\sigma}_i \delta h - 1)^2 \,. \tag{23}$$

Setting the first derivative of (23) with δh equal to zero gives

$$\frac{\partial W}{\partial(\delta h)} = 2\alpha(h + \delta h) + 2\beta(\sigma_0 + \acute{\sigma}_0 \delta h - 1)\acute{\sigma}_0 +$$

$$2p \sum_{i=1}^{8} (\sigma_i + \acute{\sigma}_i \delta h - 1)\acute{\sigma}_i = 0 \,, \tag{24}$$

and thus

$$\delta h = -\frac{\alpha h + \beta(\sigma_0 - 1)\acute{\sigma}_0 + p \sum_{i=1}^{8} (\sigma_i - 1)\acute{\sigma}_i}{\alpha + \beta \acute{\sigma}_0^2 + p \sum_{i=1}^{8} \acute{\sigma}_i^2} \,. \tag{25}$$

3.3
Introduction of approximate design sensitivity

We shall consider here to approximately estimate the stress design sensitivity $\acute{\sigma}_i$ in (25). If the principle of the virtual work is assumed to be valid at each cell, we have

$$\int_{\Omega_e} \delta \boldsymbol{\varepsilon}^T \boldsymbol{\sigma} \mathrm{d}\, \Omega = \int_{\Gamma_{e_t}} \delta \mathbf{u}^T \overline{\mathbf{t}} d\Gamma \,, \tag{26}$$

where Ω_e and Γ_e, respectively, denote the domain occupied by the updated cell e and its boundary. Approximating the physical quantities by the interpolation functions with nodal values gives

$$\delta \mathbf{U}_e^T \mathbf{K}_e \mathbf{U} = \delta \mathbf{U}_e^T \mathbf{f} \,, \quad h \mathbf{K}_e' \mathbf{U} = \mathbf{f} \,.$$

Since the specified values on the boundary are independent of h, direct differentiation of the above equation with respect to h leads to

$$\mathbf{K}'_e\mathbf{U}_e + h\mathbf{K}'_e\acute{\mathbf{U}}_e = \acute{\mathbf{f}} = \mathbf{0}\,,$$

$$\acute{\mathbf{U}}_e = -\frac{1}{h}(\mathbf{K}'_e)^{-1}\mathbf{K}'_e\mathbf{U}_e \equiv -\frac{1}{h}\mathbf{U}_e\,. \tag{27}$$

On the other hand, direct differentiation of both sides of (10) with respect to h leads to the sensitivities of the stress components with respect to h,

$$\acute{\boldsymbol{\sigma}}_e = \mathbf{DB}\acute{\mathbf{U}}_e = -\frac{1}{h}\mathbf{DBU}_e = -\frac{1}{h}\boldsymbol{\sigma}_e\,. \tag{28}$$

Equation (28) indicates that the stress sensitivities are in proportion to the magnitude of the stress $\boldsymbol{\sigma}_e$ and the reciprocal number of the thickness of the cell h. Therefore, the stress sensitivity $\acute{\sigma}_i$ in (25) can be approximated as

$$\acute{\sigma}_i = -\frac{\sigma_i}{h}\,. \tag{29}$$

Substituting (29) into (25), we have

$$\delta h = -\frac{\alpha h + \beta(\sigma_0 - 1)(-\sigma_0/h) + p\sum_{i=1}^{8}(\sigma_i - 1)(-\sigma_i/h)}{\alpha + \beta(-\sigma_0/h)^2 + p\sum_{i=1}^{8}(-\sigma_i/h)^2} =$$

$$\frac{[-\alpha h^2 + \beta(\sigma_0 - 1)\sigma_0 + p\sum_{i=1}^{8}(\sigma_i - 1)\sigma_i]h}{\alpha h^2 + \beta\sigma_0^2 + p\sum_{i=1}^{8}\sigma_i^2}\,, \tag{30}$$

where δh is estimated from the above equation and then, the thickness of the cell is updated by

$$h^{k+1} = h^k + \delta h\,, \tag{31}$$

where the superscripts k and $k+1$ mean the number of the iteration.

3.4
Property of δh with respect to penalty parameter p

Equation (30) is dependent on the penalty parameter p. The penalty parameter p should be taken to be sufficiently large in order to approximately satisfy the constraint conditions. The convergence of the iterative scheme, however, is dependent on the magnitude of the penalty parameter p and therefore, we should select an appropriate value for p.

Consider (30) at the k-th step. If the stress values of the neighbouring cells are assumed to be invariant with $\sigma_i = 1$, it follows that

$$\delta h = \frac{[-\alpha(h^k)^2 + \beta(\sigma_0 - 1)\sigma_0]h^k}{\alpha(h^k)^2 + \beta\sigma_0^2 + 8p}\,,$$

and the rule for updating the thickness is given as

$$\frac{h^{k+1}}{h^k} = \frac{h^k + \delta h}{h^k} = \frac{\beta\sigma_0(2\sigma_0 - 1) + 8p}{\alpha(h^k)^2 + \beta\sigma_0^2 + 8p}\,.$$

Figure 3 indicates the curves of the above equation for $p = 1$, 10 and 100. We notice the following features.

1. In the case of $\sigma_0 > 1$, h^{k+1} increases relative to h^k.
2. In the case of $\sigma_0 \le 1$, h^{k+1} decreases in proportion to h^k.
3. h^{k+1}/h^k increases with an decrease of p.

Especially, from the last discussion, we notice the important suggestion for the choice p.

1. If p is relatively small, h^{k+1}/h^k becomes large. The structure is greatly modified and in a result, may be destroyed.
2. If p is relatively large, h^{k+1}/h^k becomes small. The modification of the structure is so small that the convergency rate may be very slow.

From above discussions, the choice $p = 10$ seems to be the appropriate choice.

3.5
Present algorithm

The minimization algorithm is as follows.

Step 1. Input the initial data; the size of the design domain, the specified values on boundary, the number of the cells and the design conditions.
Step 2. Perform the stress analysis by the finite element method.
Step 3. Check the convergence criterion. If the criterion is satisfied, the process is terminated. If not so, the process goes to the next step.
Step 4. The thickness of each cell is updated by the stress distribution and according to the updating rule.
Step 5. Go to Step. 2.

4
Numerical examples

4.1
Example 1

Figure 4 shows the design domain. The left side of the domain is fixed and the force P is specified at the middle of the right side as shown. The parameters are shown in Table 1. In this table, σ_0 indicates the maximum stress at the initial profile. The thicknesses of all cells are equal at the initial step.

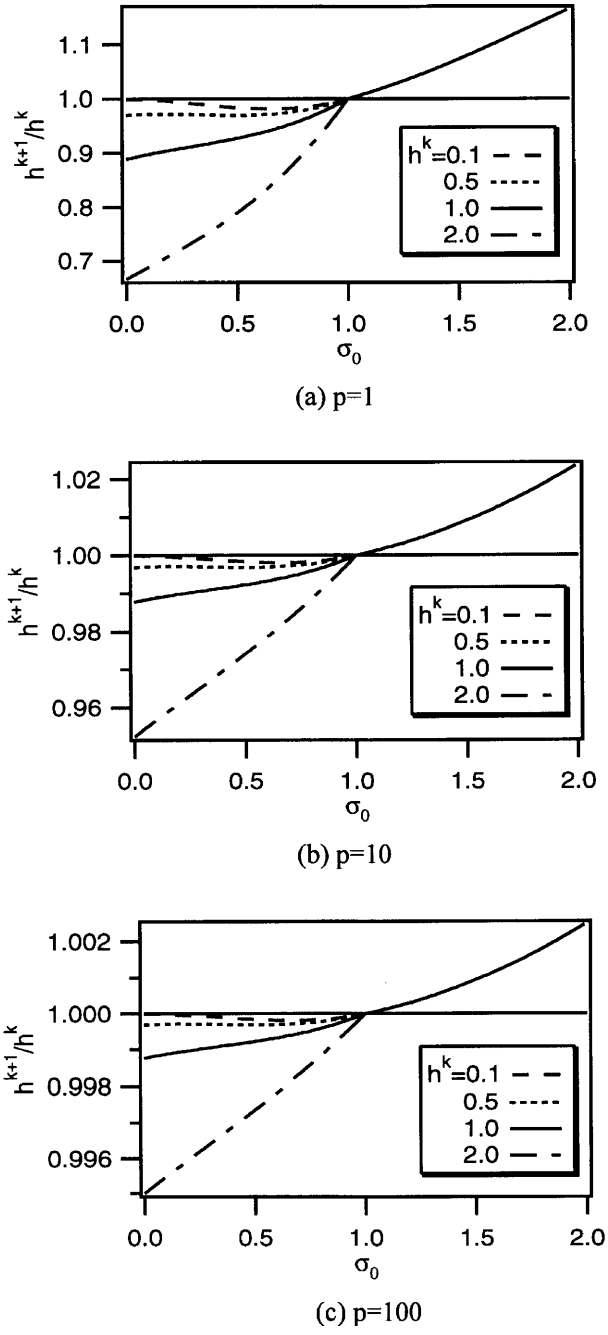

Fig. 3 δh versus σ_0 and p

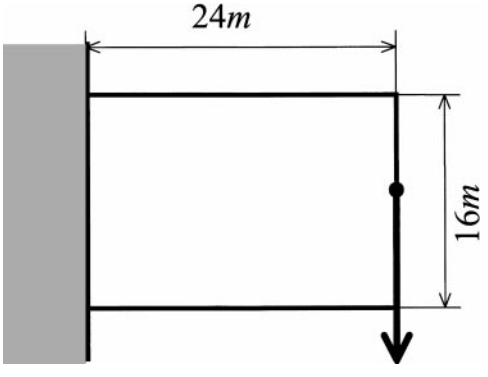

Fig. 4 Structure under consideration in Example 1

Table 1 Design parameters

Number of cells	24×16
Penalty function p	10
Young's modulus	$E = 1.0 \times 10^5$ (Pa)
Poisson's ratio	$\nu = 0.2$
Thickness of cells	$h_0 = 1.0$ (m)
Force	$P = 20.0$ (N)
Reference stress	$\sigma_c = 0.8 \times \sigma_0$

(σ_0 denotes the maximum stress at the initial profile)

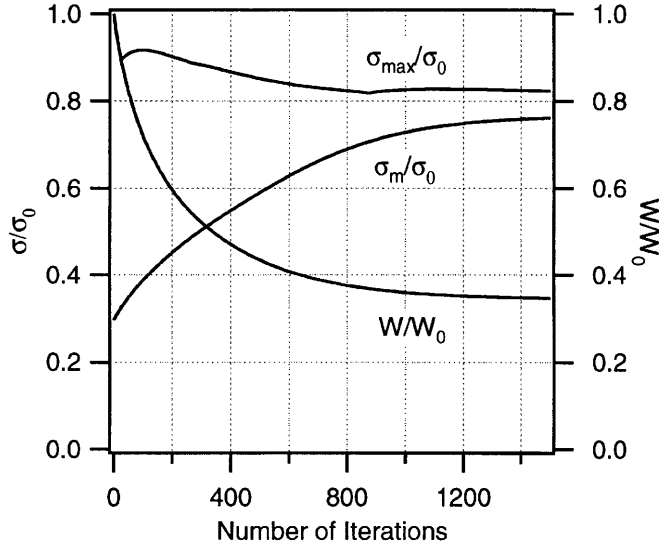

Fig. 5 Convergence histories of stresses and weight for Example 1

Figure 5 shows the convergence histories of the mean and the maximum stresses and the total weight of the structures. The maximum stress $\sigma_{\max}$ decreases rapidly when 600 iterations and then converges asymptotically to the reference stress $\sigma_c = 0.8 \times \sigma_0$. The mean stress σ_m increases gradually to the reference stress. These results indicate that the stress distribution on the whole structure tends to become uniform. Finally, the total weight of the structure decreases to 40% of its initial weight. Figure 6 shows the respective distributions of the cell thickness after 100, 400, 800 and 1500 iterations. We notice that the cells are gradually deleted from the boundary of the structure to the centre.

4.2 Example 2

A second example has the same initial profile of the previous structure but with a different load condition as shown in Fig. 8. The design parameters are the same as for Example 1.

Figure 9 shows the convergence histories of the stress and the total weight of the structure. The maximum

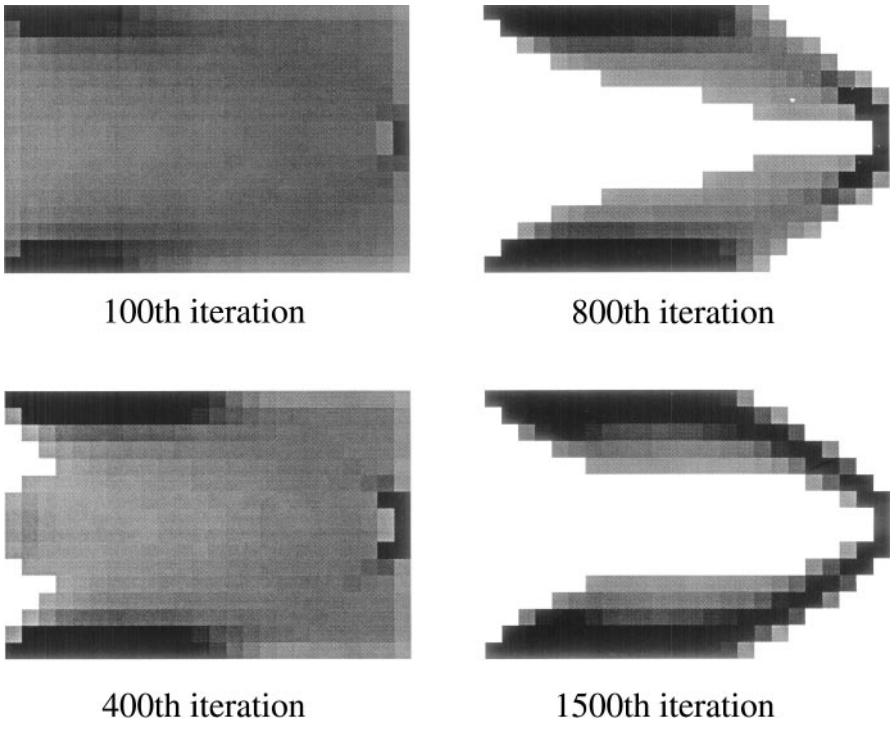

Fig. 6 Thickness distributions after different numbers of iterations for Example 1

stress $\sigma_{\max}$ decreases rapidly when 600 iterations and then converges asymptotically to the reference stress. On the other hand, the mean stress σ_m increases gradually and then, converges to half of the reference stress. We can say that here the stress distribution on the whole structure varies more than in Example 1. The total weight decreases gradually and the final structure is much lighter than that found in Example 1, about 30% of the initial weight. This is because the load point is specified in the centre of the structure and therefore the area of the structure which can be deleted is wider than that of Example 1. Figure 10 shows the distribution of the cell thickness after 100, 400, 800 and 1500 iterations. We notice that the area to the right of the load point falls away rapidly.

4.3 Example 3

For Example 3 there are two load points on the initial profile of the structure as shown in Fig. 7. The initial profile and design parameters are the same as for the previous examples.

Figure 11 shows the convergence histories of the stress and the total weight with respect to the number of the iterations. The maximum stress $\sigma_{\max}$ decreases rapidly when 600 iterations and then converges asymptotically to the reference stress. On the other hand, the mean stress σ_m increases gradually and then converges to the reference stress. Finally, the stress distribution becomes almost uniform. The total weight of the structure decreases gradually to 35% of its initial weight. Figure 12 shows the distribution of the cell thickness after 100, 400, 800 and 1500 iterations. We notice that the final profile is very similar to that found by superposing the final profiles of Example 1 and Example 2.

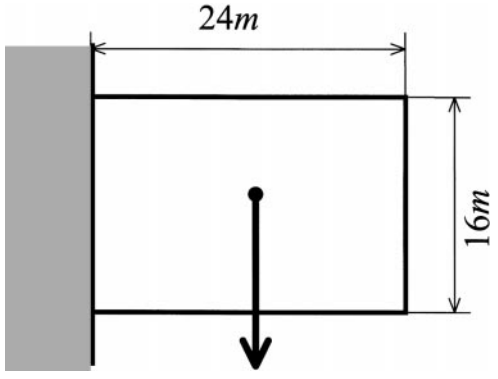

Fig. 7 Structure under consideration in Example 3

5 Conclusions

This paper presents a shape and topology optimization scheme for two-dimensional structures that uses the concept of "cellular automaton". In the existing studies, the local rule was derived from numerical experiments and therefore, was considered to be very difficult to extend

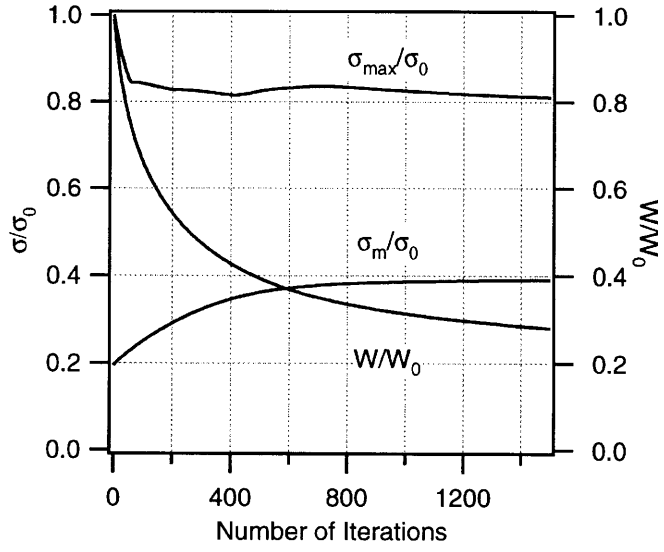

Fig. 8 Structure under consideration in Example 2

to other problems. For overcoming this difficulty, in this paper, the optimization problem is formulated at each cell by introducing the CA-constraint condition. Then, a local rule is derived by setting the first variation of the functional of the optimization problem equal to zero. Since this is based on a typical formulation of optimization problems, the physical relation between the rule and the problem is obvious. Moreover, the present scheme employs the design sensitivities. Since, however, the sensitivities are also defined between the local neighbourhood cells alone, it is not necessary to actually estimate the sensitivities. This may be an important advantage of the present scheme when comparing with the ordinary schemes which is not based on the concept of the cellular automaton.

The present scheme was applied to the shape and topology optimization of a two-dimensional elastic body. The final profiles of the structures under different load conditions are similar to the results reported in existing studies based on cellular automata concept (Inou *et al.* 1994, 1998; Kundu *et al.* 1997a,b) and using the gradient search scheme concept (Bendsøe and Kikuchi 1988; Suzuki and Kikuchi 1991). The validity of the basic idea of deriving the local rule as presented here has therefore been confirmed. Next intentions are to extend the present scheme to more complicated optimization problems and to improve the convergence rate by appropriate modification of the algorithm.

References

Bathe, K.-J. 1982: *Finite element procedures in engineering analysis*. Prentice-Hall

Bendsøe, M.P.; Kikuchi, N. 1988: Generating optimal topologies in structural design using a homogenization method. *Comp. Meth. Appl. Mech. & Engrg.* **71**, 197–224

Chaudouet-Miranda, A.; El Yafi, F. 1987: 3D optimum design using BEM technique. In: Brebbia, C.A.; Wendland, W.L.; Kuhn, G. (eds.) *Proc. Boundary Elements IX*, pp. 449–462. Comp. Mech. Pub./Springer-Verlag

Chu, D.N.; Xie, Y.M.; Hira, A.; Steven, G.P. 1998: Evolutionary topology optimization of structures subject to displacement. In: Steven, G.P.; Querin, Q.M.; Guan, H.; Xie, Y.M. (eds.) *Structural optimization* (Proc. 1st Australian Conf. on Structural Optimization, held in Sydney), pp. 419–426

Clayton, W. 1993: *Adventures in artificial life*. Que Co.

Doolen, G.D.; Frisch, U.; Hasslacher, B.; Orszag, S.; Wolfram, S. 1987: *Lattice gas methods for partial differential equations*. Reading, MA: Addison-Wesley

Eissler, W.; Drtina, P.; Frohn, A. 1992: *Trans. ASME* **61**, 1109–1114

Garzon, M. 1995: *Models of massive parallelism*. Berlin, Heidelberg, New York: Springer

Gaylord, R.; Nishidate, K. 1996: *Modeling nature: cellular automata simulations with mathematica*. Berlin, Heidelberg, New York: Springer

Guan, H.; Steven, G.P.; Xie, Y.M. 1998: Evolutionary optimization of bridge type structures. In: Steven, G.P.; Querin, Q.M.; Guan, H.; Xie, Y.M. (eds.) *Structural optimization* (Proc. 1st Australian Conf. on Structural Optimization, held in Sydney), pp. 335–342

Inou, N.; Shimotai, N.; Uesugi, T. 1994: A cellular automaton generating topological structures. In: McDonach, A.; Gardiner, P.T.; McEwan, R.S.; Culshaw, B. (eds.) *Proc. 2-nd European Conf. on Smart Structures and Materials* **2361**, pp. 47–50

Inou, N.; Uesugi, T.; Iwasaki, A.; Ujihashi, S. 1998: Self-organization of mechanical structure by cellula automata. In: Tong, P.; Zhang, T.Y.; Kim, J. (eds.) *Fracture and strength of solids. Part 2: Behaviour of materials and structure* (Proc. 3rd Int. Conf., held in Hong Kong, 1997), pp. 1115–1120

Kim, H.; Steven, G.P.; Querin, Q.M.; Xie, Y.M. 1998: Development of an intelligent cavity creation (ICC) algorithm for evolutionary structural optimisation. In: Steven, G.P.; Querin, Q.M.; Guan, H.; Xie, Y.M. (eds.) *Structural optimization* (Proc. 1st Australian Conf. on Structural Optimization, held in Sydney), pp. 241–250

Kundu, S.; Oda, J.; Koishi, T. 1997a: A self-organizing approach to optimization of structural plates using cellular automata. In: Gutkowski, W.; Mroz, Z. (eds.) *Proc. WCSMO-2, Second World Congress on Structural and multidisciplinary optimization* (held in Zakopane, Poland), pp. 173–180. Warsaw: Polish Academy of Science

Kundu, S.; Oda, J.; Koishi, T. 1997b: Design computation of discrete systems using evolutionary learning. In: Gutkowski, W.; Mroz, Z. (eds.) *Proc. WCSMO-2 , Second World Congress on Structural and multidisciplinary optimization* (held in Zakopane, Poland), pp. 173–180. Warsaw: Polish Academy of Science

Levy, S. 1992: *Artificial life, the quest for a new creation*. Penguin Books

Nha, C.D.; Xie, Y.M.; Steven, G.P. 1998: An evolutionary structural optimization method for sizing problems with discrete design variables. *Comp. & Struct.* **68**, 419–431

Payten, W.M. 1998: A fractal interpretation for optimal structures. In: Steven, G.P.; Querin, Q.M.; Guan, H.; Xie, Y.M. (eds.) *Structural optimization* (Proc. 1st Australian

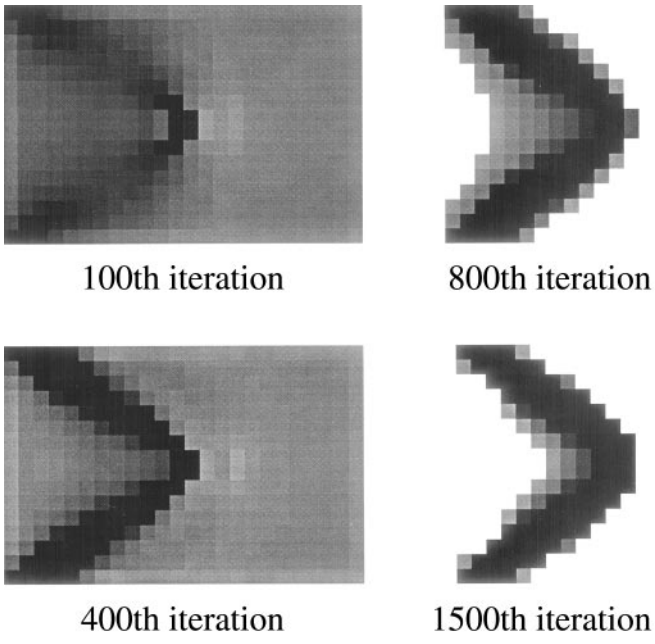

Fig. 9 Convergence histories of stresses and weight for Example 2

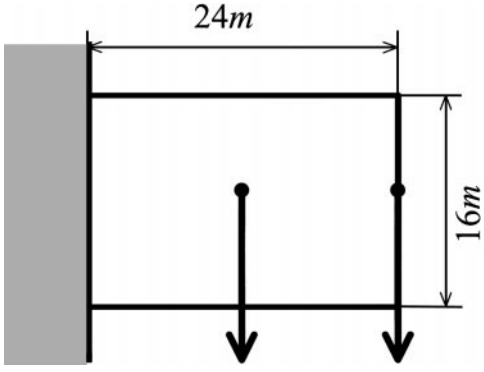

Fig. 10 Thickness distributions after different numbers of iterations for Example 2

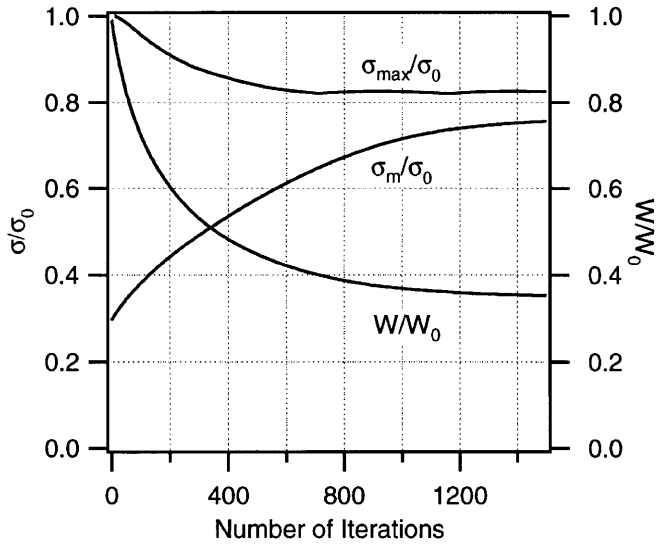

Fig. 11 Convergence histories of stresses and weight for Example 3

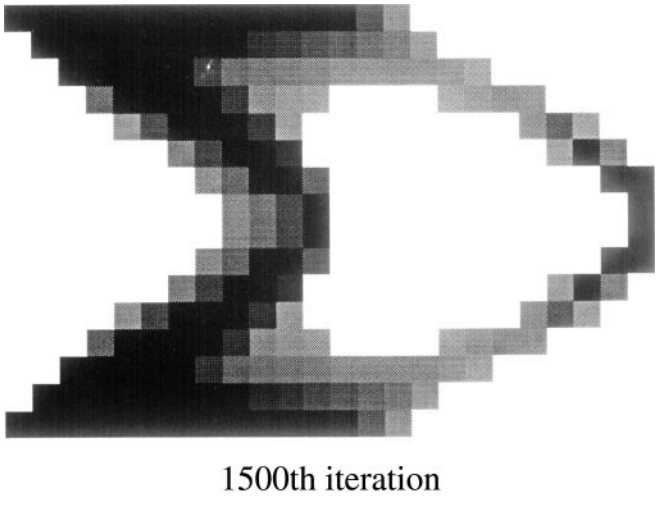

Fig. 12 Thickness distribution at final profile for Example 3

Conf. on Structural Optimization, held in Sydney), pp. 553–540

Payten, W.M.; Law, M. 1998: Topology reinforcement optimisation of flat plate and curved thin shell structures using adaptive self-organising density approach. In: Steven, G.P.; Querin, Q.M.; Guan, H.; Xie, Y.M. (eds.) *Structural optimization* (Proc. 1st Australian Conf. on Structural Optimization, held in Sydney), pp. 165–172

Payten, W.M.; Ben-Nissan, B.; Mercer, D.J. 1998: Optimal topology design using a global self-organisational approach. *Int. J. Solids Struct.* **35**, 219–237

Suzuki, K.; Kikuchi, N. 1991: Shape and topology optimization using the homogenization method. *Comp. Meth. Appl. Mech. & Engrg.* **93**, 291–318

Tada, Y.; Tadamatsu, D. 1995: Formation of structural configuration considering adaptive function of living system. *Proc. 8th Comp. Mech. Conf.*, pp. 177–178 (in Japanese)

Umetani, Y.; Hirai, S. 1975: An adaptive shape optimization method for structural material using growing-reforming method. In: *Proc. Joint JSME-ASME Applied Mechanics Western Conf.*, pp. 359–365

Waldrop, M.M. 1992: *Complexity, the emerging science at the edge of order and chaos*. Simon & Schuster

Wolfram, S. 1994: *Cellular automata and complexity*. Reading, MA: Addison-Wesley

Xie, Y.M.; Steven, G.P. 1993: A simple evolutionary procedure for structural optimization. *Comp. & Struct.* **49**, 885–896

Xie; Y.M.; Steven, G.P. 1994a: Optimal design of multiple load case structures using an evolutionary procedure. *Eng. Comput.* **11** 295–302

Xie, Y.M. Steven, G.P. 1994b: A simple approach to structural frequency optimization. *Comp. & Struct.* **53**, 1487–1491

Xie, Y.M.; Steven, G.P. 1996: Evolutionary structural optimization for dynamic problems. *Comp. & Struct.* **58**, 1067–1073

Yang, X.Y.; Xie, Y.M.; Steven, G.P.; Querin, Q.M. 1998: Bidirectional evolutionary method for frequency optimization. In: Steven, G.P.; Querin, Q.M.; Guan, H.; Xie, Y.M. (eds.) *Structural optimization* (Proc. 1st Australian Conf. on Structural Optimization, held in Sydney), pp. 231–237

Young, V.; Querin, Q.M.; Steven, G.P.; Xie, Y.M. 1998: 3D bidirectional evolutionary structural optimisation (BESO). In: Steven, G.P.; Querin, Q.M.; Guan, H.; Xie, Y.M. (eds.) *Structural optimization* (Proc. 1st Australian Conf. on Structural Optimization, held in Sydney), pp. 275–282

Zhao, C.; Steven, G.P.; Xie, Y.M. 1997: Effect of initial nondesign domain on optimal topologies of structures during natural frequency optimization. *Comp. & Struct.* **62**, 119–131

Zhao, C.; Steven, G.P.; Xie, Y.M. 1998: A generalized evolutionary method for natural frequency optimization of membrane vibration problems in finite element analysis. *Comp. & Struct.* **66**, 353–364

Zienkiewicz, O.C.; Taylor R.L. 1991: *The finite element method*. New York: McGraw-Hill